8.1 RAPID TRANSITION OF BOUNDARY LAYER STRUCTURE OBSERVED ON A COASTAL SITE

Q. Wang[1*], C. G. Helmis[2], G. Katsouvas[2], and S. Wang[3]

[1]Naval Postgraduate School, Monterey, CA
[2]University of Athens, Department of Applied Physics, Athens, Greece
[3]Naval Research Laboratory, Monterey, CA

1. INTRODUCTION

In most studies of the atmospheric boundary layer, stationarity of the turbulence field is always assumed. Based on this assumption, Monin-Obukhov Similarity Theory (MOST) or its variations are used in data analysis and interpretations. However, non-stationarity of various degrees always exists in the lower atmosphere, but it is rarely acknowledged with the exception of a few studies. Schulz and Sanderson (2004) define stationary or non-stationary based on the behavior of the flux as a function of Reynolds averaging period and found non-stationary turbulence can invalidate eddy flux calculations. They further studied a few possible indicators of stationarity such as low wind, large variation of wind direction, and significant horizontal wind variance relative to mean wind speed. McNaughton and Laubach (1998) find that non-stationarity of the wind field on the time scale comparable to surface-layer turbulence time scale modifies Bowen ratio by changing the relative magnitude of eddy diffusivity coefficients of heat and water vapor.

Under non-stationary conditions, the boundary layers constantly adjust to the changing forcing without reaching equilibrium of the turbulence field. To understand the non-stationary boundary layer, it is essential to understand how and with what time scale the adjustments are made.

Adjustment of the boundary layer turbulence also occurs in the development of the Internal Boundary Layer (IBL) formed in the presence of an advective flow through a discontinuity in roughness, temperature, heat, and moisture flux, such as a water/land interface. In many cases, solutions to the IBL problem are put into the context of the simplest possible case when two distinct semi-infinite horizontally homogeneous surfaces border each other along a straight line. This context renders the problem two-dimensional and allows us to make use of knowledge about turbulence structure and mean flow parameters in the constant-flux surface layer. One expects that, if the fetch above the new surface is long and conditions are constant, the air near the ground would be in continuous equilibrium with the new surface. The advected air from upwind and the air modified by the local surface forms an interfacial zone where intermittent turbulence may exist particularly over a short fetch (Ogawa and Ohara 1985). Between the equilibrium layer and the interfacial zone is a transition layer where the flow is not yet in equilibrium with the new surface. For a complete review of the IBL, see Garratt (1990) and Mahrt (2000).

Equilibrium between the new surface and the turbulence in the IBL is not always achieved. For example, Klipp and Mahrt (2003) found, at very short fetches, an equilibrium layer might not exist. Because of the transient variation of the level local surface driven turbulence can reach, measurements at a fix level may see intermittent periods with different turbulence characteristics as the measurement height drifts in and out of the layer with surface forced turbulence. In general, IBL studies assume stationarity and deals with the spatial variability. Even with cases of intermittently measured turbulence, averaging over long period of time can still be achieved by conditionally dividing the data into different regimes and put sections in the same regime together for statistics (Klipp and Mahrt 2003).

IBL is often found in coastal regions in both onshore and offshore flow conditions and can be grouped into several categories depending on the difference of the land surface temperature and the near-shore sea surface temperature (SST) (Mahrt 2000). Interesting enough, the coastal regions also have the most variable wind flow that results in the transient turbulent field. One good example is the onset of the sea breeze in the early afternoon when wind direction/speed changes rapidly as the sea breeze front (SBF) passes through. During the Coupled Boundary Layer Air-Sea Transfer in Low Winds (CBLAST-low) campaign in 2003, measurements at the Nantucket site documented a case with abrupt change in wind direction associated with SBF. The two levels, 10 and 20 m, on the mast with high-rate turbulence measurements indicate different time evolution of the turbulence. This paper presents some preliminary results on the evolution of the mean and turbulence field in response to the arrival of the marine air and its interaction with the local IBL. IBL development is involved since the site is about 200 m from the shoreline of the wind direction.

2. THE CBLAST NANTUCKET MEASUREMENTS

As part of the CBLAST-low efforts, we made extensive ground-based measurements on Nantucket Island, MA between July 22 and August 27, 2003. The main objectives of the measurements were to characterize boundary layers in a variety of

* *Corresponding author address:* Dr. Qing Wang, Naval Postgraduate School, Dept. of Meteorology, Monterey, CA 93940. e-mail: qwang@nps.edu

meteorological conditions and to provide in situ observations for the evaluation/improvements of mesoscale models, such as the Navy's operational forecast model, COAMPS^{TM}. Wang et al. 2004 gave a general overview of the CBLAST Nantucket measurements. Figure 1 shows a map of Nantucket coastline and the position of the CBLAST Nantucket site. The landscape surrounding the site is relatively flat except to the east and southeast due to elevated sand dunes. With the curvature of the southern coastline, the mast at the site is under marine air influence in southerly to westerly wind conditions.

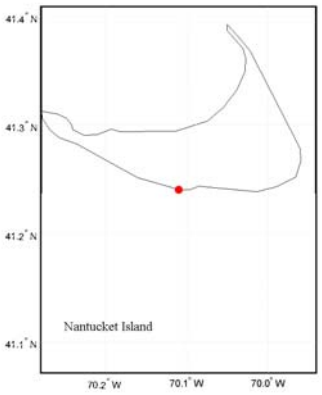

Figure 1. Coastline of Nantucket Island. The CBLAST Nantucket site is located on the tip of the south coast denoted by the red dot.

For this study, we use measurements from the 20-m mast located 94 m from the southern coastline of Nantucket Island. On the mast, there were two levels (10 and 20 m) of sonic anemometers to measure 3-D wind components and virtual temperature. At 20-m level, a LICOR fast hygrometer also measured water vapor and CO_2 concentration. These 20 Hz sampled measurements yield momentum and sensible heat fluxes at both levels, and latent heat and CO_2 fluxes at 20 m using the eddy correlation method. The mean wind, temperature, and relative humidity (RH) were also measured on the mast at 5, 10, and 20 m levels at 10-minute sampling interval. Nearby the 20-m mast (about 10 m to the north), a small tripod was setup to measure air temperature, RH, wind speed and direction, air pressure, and precipitation at 1-minute interval. The sensor height was set at about 2 m. Since the tripod and the mast were very close to each other, their measurements are considered at the same location. We therefore have measurements of mean quantities at four levels at the site.

The Nantucket instrument suite also included a Remtech (PA2) SODAR system for probing the lower atmosphere. The SODAR system resulted in vertical profiles of the horizontal wind speed and direction, the echo strength, the vertical (w), the standard deviations of the three wind components, the momentum fluxes ($\overline{w'u'}$ and $\overline{w'v'}$), and the atmospheric static stability class (four categories) at 30-minute intervals. The vertical resolution of the profiles is 40m and ranged up to 600 m. More details regarding SODAR system and its parameters can be found in Helmis *et al.* (2004). Helmis *et al.* (2006) presents an analysis on the inertial oscillation in the stable boundary layer using the SODAR measurements. In addition, rawinsondes were launched two to six times daily in coordination with other CBLAST activities. We also experimented with tethered rawinsondes (without wind measurements) that went up to 200 m above ground on two days during the intensive observational period. These tethered soundings at short time intervals were designed to study the rapid evolution of boundary layer thermodynamic structure, particularly the development of the internal boundary layers. All data have gone through extensive data quality checking and calibrations.

3. EVOLUTION OF THE MEAN THERMODYNAMICS QUANTITIES

This study focuses on the measurements from August 14, 2003. The sea breeze onset on this day is identified by sharp changes of wind direction at several CBLAST measurement sites around 13:46 (LST). Figure 2 shows the measurements of wind and the Corresponding variation in low-level potential temperature (θ), RH, specific humidity (q), and CO_2 concentration for the entire day at four measurement levels: 2, 5, 10, and 20 m. Between midnight and the early morning, the 2- and 5-m are nearly identical in all variables, suggesting that the two lowest levels are in a well-mixed layer, while the layer between the 5 and 20 m levels is in stable stratification as seen by the higher θ at 20 m compared to 5 m. At around 5 AM, near surface temperature increases and quickly becomes

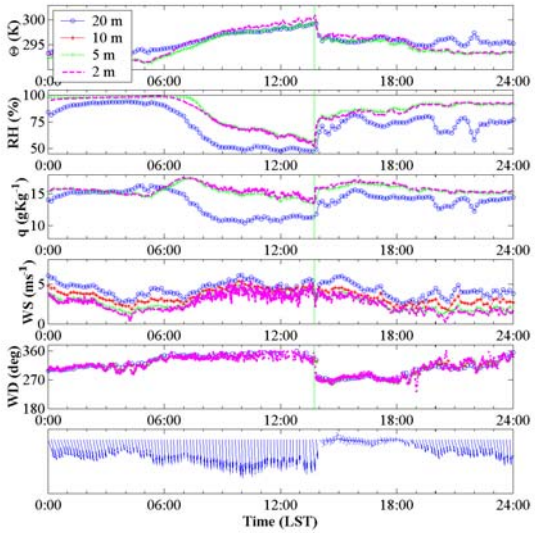

Figure 2. Diurnal variation of mean variables sampled at 10-minute intervals. The lowest panel shows the wind vector where the direction of the arrows points to the direction wind is heading.

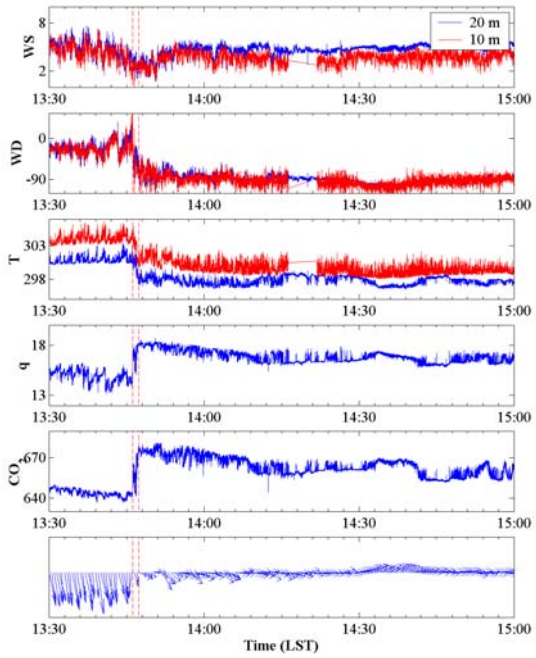

Figure 3. Variations of wind speed, direction, temperature, specific humidity, and CO_2 concentration near the time of SBF passage.

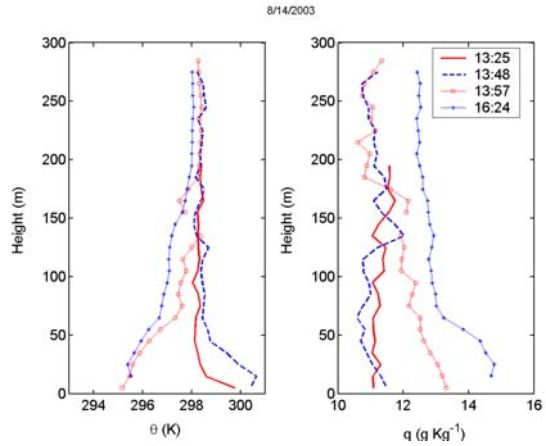

Figure 4. Vertical profiles of potential temperature and specific humidity near the time of SBF passage. The legend denotes the average time around which the sounding was made.

the same or higher than the 20 m θ. These vertical thermodynamic structure and their time evolution are typical of the diurnal variation over land in northerly wind conditions (land surface boundary layer). At 13:46 (LST), wind direction change quickly from northerly to westerly. At the wind direction change, θ drops about 2.7 K from 299.4 K to 296.7 K, q increases by 2.1 g kg^{-1} at 2 and 5 m and 1.6 gkg^{-1} at 20 m (instrument malfunction was found at the 10 m level). We also notice, from the wind speed, that the vertical wind shear between 10 m and 20 m increases after the SBF passes. Since the slow sensors measured the mean quantities in 10-minute intervals, the data are too coarse to pinpoint the onset of what appears to be rather sharp changes; the time series of the corresponding variables from the fast sensors are further examined in Fig. 3. The vertical dash lines in Fig. 3 denote the transition period from the land air to the marine air, which is well defined in the time series of temperature and CO_2 concentration. This transition in mean field happened in less than 1.5 minutes (13:46:12 to 13:47:24 LST) at both 10 and 20 m heights. The beginning of this transition (13:46:12 LST) is considered as the time marine air arrived at the site. We will also refer to this moment as the time of sea breeze onset at this location. We also notice the gradual decrease in q and CO_2 following the initial jump. Specific humidity and CO_2 becomes level off after about 26 minutes.

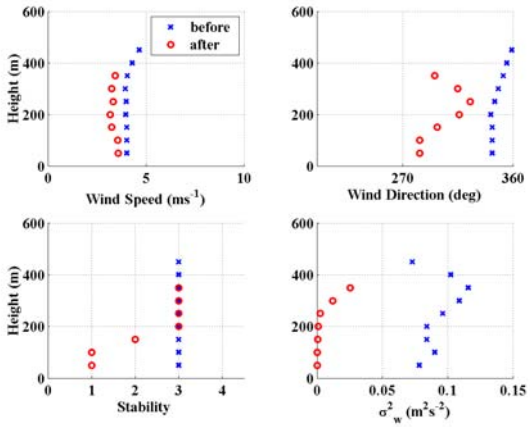

Figure 5. Vertical profiles of wind speed, direction, stability category, and the variance of vertical velocity from the Remtech SODAR. Stability category 1 through 4 represent stable, weakly stable, neutral, and weakly unstable, respectively.

The tether sonde measurements on Aug. 14 2003 capture the variation in boundary layer vertical structure before and after the passage of the SBF. Figure 4 shows the drastic change of the thermal stratification as SBF passes by the site from four successive soundings. The most significant change occurs between two soundings about 9 minutes (from 13:48 to 13:57 LST) apart. Comparison of these two soundings shows that the largest change occurs below 60 m where the strongly unstable stratification changed to a surface-based inversion. Between 60 and 130 m above surface, the layer remains well mixed after the transition at 1 K lower temperature. No change was observed above the 130 m level. Thus the sea breeze may have only extended up to 130 m above ground.

The SODAR measured vertical profiles of wind, stability, and turbulence (vertical velocity variance) is shown in Figure 5. They show that wind direction

change mainly occurs below about 150 m. In this layer, there are corresponding changes in the thermal stability from neutral (category 3) to stable (category 1). Vertical velocity variance decreased most significantly to nearly zero in the lowest 200 m, although it also decreased in the layer above. These results seem to be consistent with the tether sonde measurements.

4. EVOLUTION OF THE LOW-LEVEL TURBULENCE

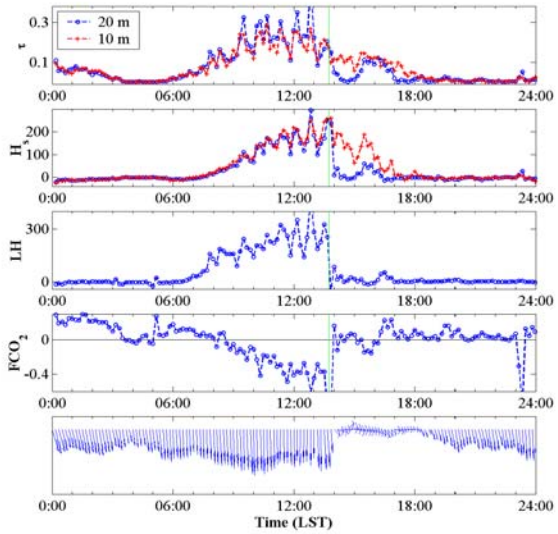

Figure 6. Diurnal variations of turbulent momentum flux (τ, in Nm^{-2}), sensible heat flux (H_s, in Wm^{-2}), latent heat flux (LH, in Wm^{-2}), and flux of CO_2 (FCO_2, in $mgm^{-2}s^{-1}$). The vertical dash lines show the time of sea breeze onset at the site.

Figure 6 shows the turbulent fluxes of momentum, sensible, latent, and CO_2 fluxes on Aug. 14, 2003. These fluxes were obtained using eddy correlation method averaged over 10-minute intervals. Diurnal variation of the turbulence fluxes shows a typical evolution over a land surface boundary layer during the northerly wind period. Particularly, the fluxes at 20 and 10 m are nearly the same, suggesting that both are in the constant-flux surface layer. The 20-m fluxes decrease sharply after the SBF passage while no significant drop is seen at the 10-m height. This is different from the mean quantities where adjustments happen at all levels. Close inspections of the 10-m fluxes reveal the asymmetry of the time evolution in the early afternoon after the transition compared to the morning evolution implying that the change in wind direction also affects the 10 m turbulent fluxes. Our spectra analysis presented in a later section reveals that the 10-m height is within the local IBL. Beginning at 14:37, about 1 hour after the SBF passage, fluxes at 20 m height increases. The momentum flux increases to nearly the same as that at the 10 m height, which is an indication that the 20 m level is now in the IBL as the 10 m level.

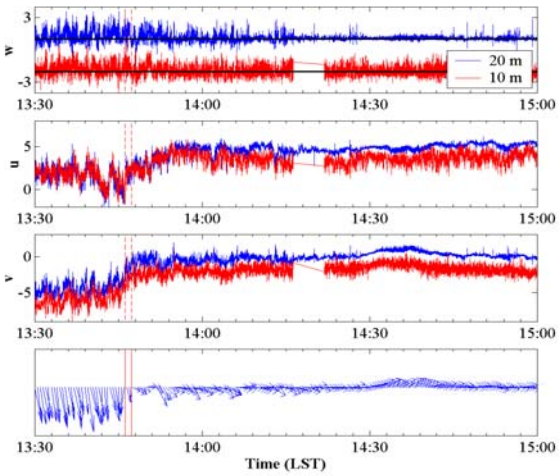

Figure 7. Time evolution of turbulence after the SBF passage. The vertical velocity (w) is adjusted by 1 ms^{-1} and –2 ms^{-1} (the thick black lines) to the 20-m and 10-m data, respectively, to prevent overlapping in the figure. The v wind component is also adjusted by adding 1 ms^{-1} to the 20-m data. All velocities are in unit of ms^{-1}.

Figure 7 shows the variation of the turbulence perturbations within approximately an hour after the SBF passage. The two vertical dash lines are the same as those in Fig. 3 to denote the time period within which the mean quantities adjusted to the new air mass from the water. From the 20-m measurements, we clearly see the gradual decrease of the turbulence intensity in all three components of the wind after the onshore flow. However, the adjustment of the turbulence field goes much slower compared to that of the mean field. No obvious adjustment in the intensity of the 10-m turbulent field can be visually identified.

In order to quantify the adjustment of the turbulence field, we examine the variation of turbulent kinetic energy. However, due to the transient nature of the turbulence seen in Fig. 7, it is inappropriate to choose a long time series for Reynold's averaging. With a shorter dataset, on the other hand, we may encounter the problem of insufficient statistical representations. This is a well-recognized data analysis issue in transient conditions. Without effective innovative analysis techniques whose existence is unclear from the current literatures, we still attempt to use a shorter data length with the knowledge that our statistics may not be the most appropriate. A test is performed with this specific dataset to examine the impact of a shorter dataset (Fig. 8). Figure 8 compares TKE obtained using 10-minute averaging with that using 2-minute averaging for both 10-m and 20-m measurements. Expectedly, the 2-minute averaging shows larger variability of the resultant TKE. In the northerly wind period, the 2-minute averaging can underestimate TKE by as much as 30%. After the SBF passage, no significant difference in the

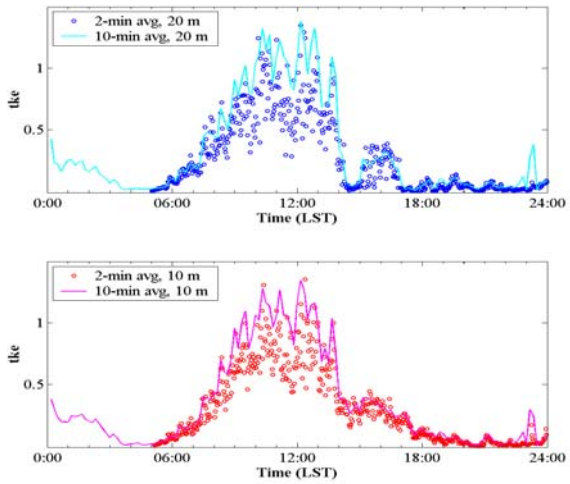

Figure 8. A comparison of TKE obtained using 2-minute averaging vs. 10-minute averaging. TKE is in unit of m^2s^{-2}.

mean TKE can be seen, particularly during the period of transient turbulence after 13:46 LST. Hence, a 2-minute averaging scheme is used to further study the time evolution of TKE during the transition period (Fig. 9). Figure 9 shows that turbulence become steady at a very low level at around 14:18 (LST). Results in Fig. 9 will be the basis for estimating the TKE storage term ($\partial e/\partial t$) as part of a TKE budget analysis planned for the future. The TKE budget analysis, in comparison with the mean budget analysis, should reveal the difference of time response between turbulence and the mean quantities. Our hypothesis is that the horizontal advection following the SBF passage dominates in the budget of the mean quantities, whereas in the budget of TKE, shear and buoyancy production terms are likely comparable to the advection of TKE, resulting in a smaller storage term.

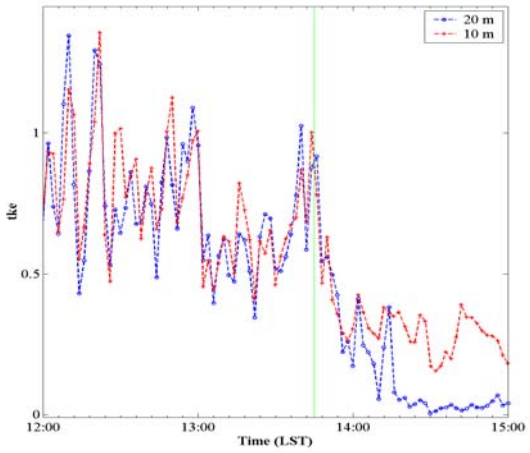

Figure 9. Variation of TKE (tke, in m^2s^{-2}) after the SBF passage at 10 and 20 m heights. The vertical line denotes the onset of wind direction change.

5. SPECTRAL CHARACTERISTICS DURING THE TRANSITION PERIOD

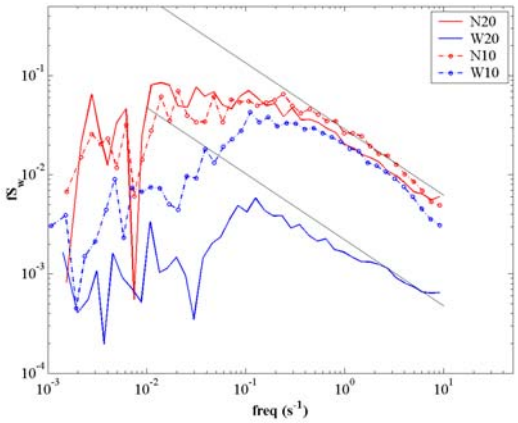

Figure 10. Power spectra of vertical velocity from different time periods at 10-m and 20-m heights. The straight lines have a –2/3 slope on the log-log plot.

This section will focus on the evolution of the turbulence spectra prior and after the SBF passage. To study the time evolution of the turbulence scales, we separate the measurements into different time periods, the northerly wind, westerly wind, and the transition periods denoted by a prefix of 'N', 'W', and 'T', respectively. These periods represent the time before, after when turbulent statistics becomes steady, and the transient period after the SBF passage. To deal with the transient period, we further separate the period into three subsections denoted as 'T201', 'T202', and 'T203' for the 20-m measurements. With the assumption that the time scale of the turbulence adjustment is longer than the length of the subsections so that turbulence can be treated as stationary within each subsections.

Figure 10 shows a comparison between the w power spectra during the two steady periods using 10-m and 20-m measurements. In the northerly wind section, the power spectra from the two levels are nearly identical with a peak frequency of about 0.013 s^{-1}. Using a 5 m s^{-1} mean wind and Taylor's hypothesis, the corresponding peak wavelength is about 380 m, which is about the depth of the mixed layer seen from the SODAR sounding profiles (Fig. 5). In the steady westerly wind period, the magnitude of power spectra at 10-m height decreases only slightly from the northerly wind period. However, the peak frequency is much larger (0.176 s^{-1}), which translates into a peak wavelength of 21 m with a mean wind speed of 3.7 ms^{-1}. This change in peak wavelength signals that the 10 m level is in a newly formed IBL in the onshore wind conditions and the IBL depth is on the order of 21 m.

The spectra in the steady westerly wind period at 20 m deceases sharply and the inertial subrange is not as clearly defined as in the other time periods/levels. The peak frequency is at 0.107 s^{-1} corresponding to a spatial scale of 37 m using a leg averaged mean wind speed of 5.1 m s^{-1}. The 20-m level is likely in the transition zone between the IBL and the marine air above.

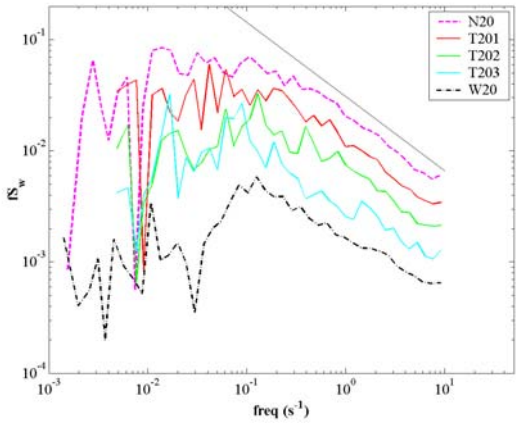

Figure 11. Power spectra of vertical velocity from different time periods at 20 m height. The straight line has a –2/3 slope on the log-log plot.

Figure 11 shows the evolution of the turbulence power spectra at the 20-m level. Note that the three periods in the transition regime have shorter data length and hence cannot resolve the lower frequencies compared to the two stationary regimes (N20 and W20). The spectra show more variations compare to the two steady regimes. The transition to smaller and smaller turbulence eddy scales with less TKE is evident from this figure. The destruction of the inertial subrange is also observed as the decay of turbulence progresses.

6. CONCLUSIONS

Detailed analyses on the variation of mean and turbulence statistics have been made using measurements from the CBLAST Nantucket site on a unique case when the sea breeze front passes over the site. As a result of abrupt wind direction change, the near-surface temperature, specific humidity, and CO_2 concentration changes from the previous over-land air to marine air properties in less than 1.5 minutes. However, it is found that the turbulence field responds to the change with a much longer time scale, about 32 minutes (13:46-14:18 LST). Further analyses of the turbulent spectra also reveal the development of an IBL after the SBF passage that contributes to the different behavior of turbulence adjustment at 10 and 20 m. The 20-m level was likely in the interfacial layer between the newly developed IBL and the marine air above, while the 10-m level was within the IBL in equilibrium with the local surface. Further analysis of TKE budget and budget of the mean quantities should provide more insight into the adjustment time scales and will be the subject of future study.

7. ACKNOWLEDGEMENTS

We thank Dr. Zhiqiu Gao for his efforts in initial data processing and Dr. Kostas Rados in analyses of COAMPS results to understand the onset of sea breeze. We also thank Dr. Jim Edson for his efforts in making the surface met observations co-located with our in situ and remote sensors and provided us the calibrated data from the 2-m tripod. Dr. John Kalogiros provided many useful MATLAB tools for data processing. This research was supported by the Office of Naval Research (ONR) for the CBLAST project.

8. REFERENCES

Garratt, J. R.: 1990, 'The Internal Boundary Layer – A Review', *Boundary-Layer Meteorol.* , **50**, 171–203.

Helmis C.G., Wang, Q., Halios, C.H., Wang, S., and Sgouros, G.: 2004, On the vertical turbulent structure of the Marine Atmospheric Boundary Layer, 16th Symposium of the AMS on Boundary Layers and Turbulence, Portland, ME, 9-13 August.

Helmis C.G., Wang, Q., Halios, C.H., Sgouros, G., and Wang, S.: 2006, " Frictional decoupling and the intertial Oscillation in stable marine atmospheric boundary layer, CD Distribution, 27th Conference on Hurricanes and Tropical Meteorology, 24–28 April 2006, Monterey, CA.

Klipp, C., and Mahrt, L.:, 2003, Conditional Analysis of an Internal Boundary Layer, *Boundary-Layer Meteorol.* , **108**, 1–17.

Mahrt, L.: 2000, Surface Heterogeneity and Vertical Structure of the Boundary Layer, *Boundary-Layer Meteorol.* , **96**, 33–62.

McNaughton, K. G. and Laubach, J.: 1998, 'Unsteadiness as a Cause on Non-Equality of Eddy Diffusivities for Heat and Vapour at the Base of an Advective Inversion', *Boundary-Layer Meteorol.* , **88**, 479–504.

Ogawa, Y. and Ohara, T.: 1985, 'The Turbulent Structure of the Internal Boundary Layer near the Shore, Part 1', *Boundary-Layer Meteorol.*, **31**, 369–384.

Schulz, E.W and Sanderson, B.G.: 2004, Stationarity of Turbulence in Light Winds during the Maritime Continent Thunderstorm Experiment, *Boundary-Layer Meteorol.* , **111**, 523-541.

Sorbjan, Z.: 1989, *Structure of the Atmospheric Boundary Layer*, Prentice Hall, Englewood Cliffs, NJ, 317 pp.

Wang Q., Helmis, C.G., Gao, Z., Kalogiros J.A., and Wang, S.W.: 2004: "Variations of Boundary Layer Turbulence and mean Structure using synthesized Observations", *16th Symposium of the AMS on Boundary Layers and Turbulence*, Portland, ME, 9-13 August.